# Stimulated X-Ray Emission Spectroscopy in Transition Metal Complexes

Thomas Kroll, Clemens Weninger, Roberto Alonso-Mori, Dimosthenis Sokaras, Diling Zhu, Laurent Mercadier, Vinay P. Majety, Agostino Marinelli, Alberto Lutman, Marc W. Guetg, Franz-Josef Decker, Sébastien Boutet, Andy Aquila, Jason Koglin, Jake Koralek, Daniel P. DePonte, Jan Kern, Franklin D. Fuller, Ernest Pastor, Thomas Fransson, Yu Zhang, Junko Yano, Vittal K. Yachandra, Nina Rohringer, and Uwe Bergmann

Phys. Rev. Lett. **120**, 133203 — Published 27 March 2018
DOI: 10.1103/PhysRevLett.120.133203

# Stimulated X-ray Emission Spectroscopy in Transition Metal Complexes

Thomas Kroll[1,2],[*] Clemens Weninger[3,1],[†] Roberto Alonso-Mori[1], Dimosthenis Sokaras[2], Diling Zhu[1], Laurent Mercadier[3], Vinay P. Majety[3], Agostino Marinelli[4], Alberto Lutman[4], Marc Guetg[4], Franz-Josef Decker[4], Sébastien Boutet[1], Andy Aquila[1], Jason Koglin[1], Jake Koralek[1], Daniel P. DePonte[1], Jan Kern[1,5], Franklin D. Fuller[5], Ernest Pastor[5], Thomas Fransson[6], Yu Zhang[6], Junko Yano[5], Vittal K. Yachandra[5], Nina Rohringer[3,7,8],[‡] and Uwe Bergmann[1,6§]

[1] *LCLS, SLAC National Accelerator Laboratory, Menlo Park, CA 94025, USA*

[2] *SSRL, SLAC National Accelerator Laboratory, Menlo Park, CA 94025, USA*

[3] *Max Planck Institute for the Structure and Dynamics of Matter, 22761 Hamburg, Germany.*

[4] *Accelerator Directorate, SLAC National Accelerator Laboratory,Menlo Park, CA 94025, USA*

[5] *Molecular Biophysics and Integrated Bioimaging Division, Lawrence, Berkeley National Laboratory, Berkeley, CA 94720, USA*

[6] *Stanford PULSE Institute, SLAC National Accelerator Laboratory, Menlo Park, CA 94025, USA*

[7] *DESY - Deutsches Elektronen Synchrotron, 22607 Hamburg, Germany.* and

[8] *University of Hamburg, 22761 Hamburg, Germany.*

(Dated: February 13, 2018)

# Abstract

We report the observation and analysis of the gain curve of amplified K$\alpha$ X-ray emission from solutions of Mn(II) and Mn(VII) complexes using an X-ray free electron laser to create the 1s core-hole population inversion. We find spectra at amplification levels extending over four orders of magnitude until saturation. We observe bandwidths below the Mn 1s core-hole lifetime broadening in the onset of the stimulated emission. In the exponential amplification regime the resolution corrected spectral width of $\sim$1.7 eV FWHM is constant over three orders of magnitude, pointing to the build-up of transform limited pulses of $\sim$1 fs duration. Driving the amplification into saturation leads to broadening and shift of the line. Importantly, the chemical sensitivity of the stimulated X-ray emission to the Mn oxidation state is preserved at power densities of $\sim 10^{20}$ W/cm$^2$ for the incoming X-ray pulses. Differences in signal sensitivity and spectral information compared to conventional (spontaneous) X-ray emission spectroscopy are discussed. Our findings build a baseline for nonlinear X-ray spectroscopy for a wide range of transition metal complexes in inorganic chemistry, catalysis and materials science.

X-ray free-electron (XFEL) sources [1, 2] provide X-ray pulses of femtosecond and potentially attosecond duration [3] of unprecedented high-intensities [4] and could become game changers for X-ray spectroscopy applications. Current experiments are using primarily the linear interaction of matter with the X-ray pulses taking advantage of their ultrashort duration [5, 6]. However, given the ultrahigh intensities that can be obtained when focusing these pulses, nonlinear X-ray matter interaction can also occur [7–11]. An exciting future perspective is the transfer of nonlinear spectroscopy from the optical to the X-ray spectral region [12–15]. Here, one can envision tuning two or more X-ray pulses to inner-shell ionization edges or resonances of particular atomic constituents in the sample, creating an element sensitive, local probe. Phase matching geometries in such setups could result in directed, background free emission of a nonlinear signal, encoding a particular component of the nonlinear polarization of the system under study. Moreover, nonlinear spectroscopy may provide a way to differentiate between inhomogeneous and homogeneous line broadening [16], and metal centers could be sensitively probed by such techniques in a coherent manner to unravel long-range charge and energy transfer processes [17, 18]. In particular 3d transition metals play a critical role in many of these processes and are also at the heart of many catalytic reaction centers. While these experimental techniques are currently still out of reach, our work presented here is a first step towards the spectroscopic use of nonlinear X-ray methods for the chemical analysis of 3d transition metal systems.

As a conventional (linear) X-ray probe of 3d transition metals, core-to-core X-ray emission spectroscopy (XES) after 1s ionization, such as 2p → 1s (K$\alpha$) and 3p → 1s (K$\beta$), encode the effective oxidation and spin state [19, 20], resulting in characteristic shifts ('chemical shifts') of the emission spectra. XES has been successfully applied to characterize the electronic and geometric structure of 3d transition metal complexes [21, 22] and expanding XES into the nonlinear regime will further enhance our understanding of these systems. Two of the basic phenomena of nonlinear X-ray spectroscopy are amplified spontaneous emission and impulsive stimulated X-ray scattering. Both have been demonstrated in atomic gases resulting in a directed emission of the X-ray signal in a laser-like beam and coherent amplification factors of up to $10^8$ [23, 24]. The onset of amplified spontaneous emission was recently observed in the condensed phase in the VUV regime [25] (amplification factors of 2) and hard X-ray regime [13] (amplification factors of 10). These proof-of-principle experiments aimed for first demonstration of these stimulated X-ray emission effects, but did not focus on spectroscopy aspects. Here, we present the observation of amplified spontaneous K$\alpha$ emission of Mn compounds in aqueous solution and the quantitative study of its gain curve and spectroscopic features. Throughout the paper we refer to this phenomenon simply as stimulated X-ray emission or stimulated emission.

Stimulated X-ray emission requires very bright X-ray pump pulses, which at present are based on self-amplified spontaneous emission (SASE) XFEL sources [1, 2]. The stochastic SASE process produces a sequence of spikes of highly fluctuating intensity, both in the spectral and temporal domain. This results in pulses of limited temporal coherence, thus impeding the experimental control and analysis. To measure stimulated emission driven by a stochastic source, high gain and optically dense samples are necessary [26, 27]. In order to become a valuable spectroscopic technique, the spectral evolution at these high gain conditions have to be understood and examined. One of the central question is if valuable chemical information remains preserved at these extreme X-ray pump intensities. This has motivated our study of stimulated K$\alpha$ X-ray emission from two chemically distinct Mn compounds in aqueous solutions, Mn(II)$Cl_2$ and NaMn(VII)$O_4$.

Experiments were performed at the Coherent X-ray Imaging (CXI) instrument [28] at the Linac Coherent Light Source (LCLS) at SLAC National Accelerator Laboratory [1]. The experimental setup is sketched in Figure 1a. The 10-30 fs long incoming X-ray pulses were tuned to a photon energy of 6.6 keV. They were focused onto a liquid jet with a thickness of 200 $\mu$m at the beam interaction with an estimated spot size of $\sim$150 nm diameter [29]. The stimulated X-ray emission spectra were analyzed using Bragg reflextions from flat Si perfect-crystals and a position sensitive 2d detector [30]. Spontaneous XES spectra of the 5M $MnCl_2$ and 4M $NaMnO_4$ solution samples were recorded at the Stanford Synchrotron Radiation Lightsource (SSRL) at beamline 6-2 [31]. Theoretical spontaneous XES spectra of were obtained using charge transfer multiplet calculations [32–35]. Details are given in the Supporting Material.

We create stimulated X-ray emission by photoionization of inner-shell electrons [36] in a quasi gain-swept geometry [37–39]. Specifically, the X-ray beam generates a short lived core-excited state $1s^1 2p^6 3d^n$ (n=5 for $MnCl_2$, n=0 for $NaMnO_4$) leading to a population inversion inside a volume created by the incident XFEL pulse (filled circles in Figure 1b). Part of these excited ions decay spontaneously to a $1s^2 2p^5 3d^n$ final state configuration, isotropically emitting K$\alpha$ fluorescence. Spontaneously emitted photons propagating in the

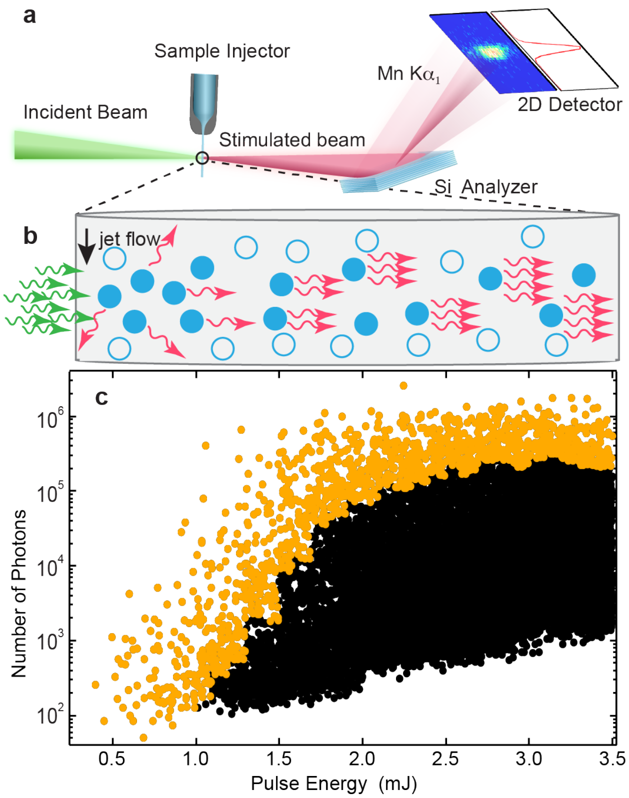

FIG. 1. a: Experimental setup. The incoming XFEL pulses are focused onto the liquid jet. The simulated X-ray emission is detected using a flat analyzer crystal and a position sensitive 2d detector. b: Sketch of stimulated X-ray emission. The arrows represent incoming (green) and emitted (red) photons, while the circles indicate the excited participator (filled) and spectator (open) Mn ions respectively. c: Detected number of photons in the Mn K$\alpha_1$ region (5 eV integration window) as a function of the nominal incoming XFEL pulse energy for the 5M MnCl$_2$ solution. The actual pulse energy on target is ∼20% of the nominal pulse energy shown in the figure. The 50 strongest shots in each 0.1 mJ interval are shown in yellow, all other shots in black.

forward direction along with the XFEL pulse can stimulate emission along the inverted medium. This results in exponential amplification of the initial fluorescence photons and generates an intense self-seeded stimulated emission pulse in forward direction, as sketched out in Figure 1b [40]. This is shown in Figure 1c, where we plot the measured stimulated K$\alpha$ emission intensity per shot versus the incident pulse energy on a logarithmic scale, after filtering the signal with the Si analyzer. An exponential increase of the maximum intensity is observed until ∼2 mJ, after which the signal saturates with a maximal number of $10^6$ measured photons in a single shot, corresponding to $4 \times 10^7$ generated photons according to the 2.5% efficiency of our analyzer. The gain curve shows strong variations in the stimulated emission strength extending over several orders of magnitude for a given XFEL pulse energy (see discussion below). To illustrate the gain curve limit, the top 50 strongest shots in each 0.1 mJ interval are shown in yellow.

We find an onset of saturation of the experimental gain curve (bending of the curve) at $2 \times 10^5$ detected photons. Taking into account the 2.5% analyzer efficiency, an estimated source diameter of 150 nm and a stimulated emission pulse duration of ~1 fs, this measured photon output at saturation corresponds to a saturation intensity of $\sim 4 \times 10^{16}$ W/cm$^2$. This experimental value of the saturation intensity can be compared to a simple gain model of transient X-ray lasers [41], for which the saturation intensity is determined by equating the stimulated emission rate with the decay rate (Auger and fluorescence rate) of the core-excited state. In our case, the decay width of the core hole excited state is 1.16 eV and the K$\alpha$ width of 1.48 eV [42]. Using these values to calculate the stimulated emission cross section we find a saturation intensity of $\sim 10^{17}$ W/cm$^2$. Given the simplicity of the model this is value is reasonably close to our experimentally observed value of $\sim 4 \times 10^{16}$ W/cm$^2$. The strongest recorded shot was measured at an XFEL pulse energy of 2.4 mJ, for which $2 \times 10^6$ photons were detected. Correcting for the ~2.5% analyzer efficiency, this translates to $\sim 8 \times 10^7$ photons emitted by stimulated emission. To estimate the amplification factor over spontaneous emission we attenuated the incoming beam to 8% to avoid stimulated emission and measured the spontaneous emission for 30 minutes. We observed a signal rate of 0.08 photons/pulse for the K$\alpha_1$ spectrum, which, correcting for this attenuation, corresponds to ~ 1 photon per pulse. Comparing this number to the strongest measured stimulated emission shot corresponds to an amplification factor of $\sim 2 \times 10^6$ (as both measurements used the same ~2.5% efficient analyzer). Our amplification gain findings go well beyond previous data [13], which showed the onset of stimulated emission in Cu foils with a gain of approximately one order of magnitude.

There are several contributions that cause the strong variations observed in the stimulated emission intensity (Figure 1c). One of them comes from the stochastic nature of the stimulated emission process. Additional contributions are caused by the inherent shot-to-shot SASE fluctuations and the pointing instability of the XFEL onto the beam-transport and focusing optics. There might also be some fluctuations of the sample thickness caused by incomplete reformation of the jet after being disrupted in the previous pulse. Further-

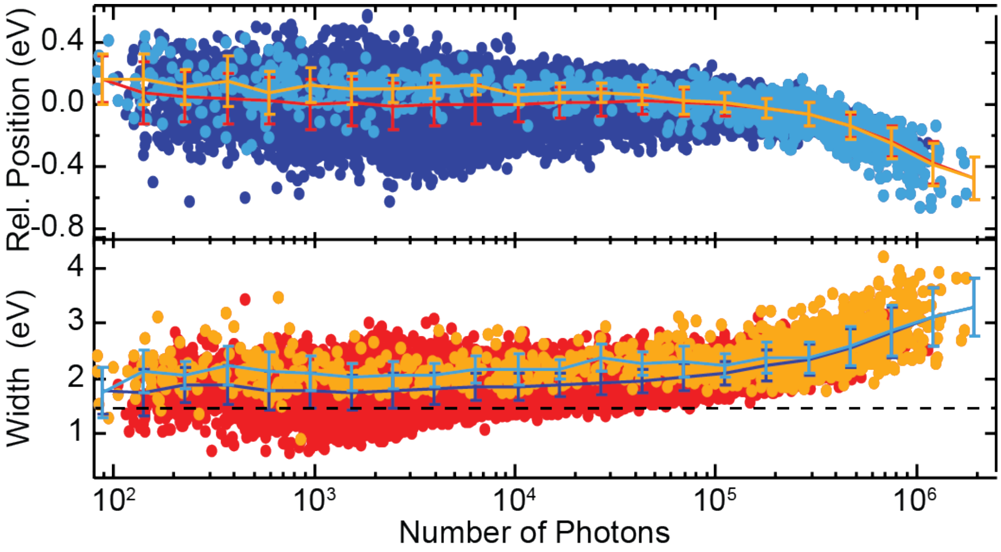

FIG. 2. Relative position (top) and width (bottom) of the stimulated XES peak as a function of the number of detected photons in the emission line. The bright colors represent the selected shots given in yellow in Figure 1c. Both position and width are constant within error bars up to a peak intensity of $\sim 2\times10^5$ detected emission photons per shot, before they get broader and shift towards lower emission energies. The dashed line represents the natural lifetime broadening of 1.48 eV.

more, each SASE XFEL pulse consists of a temporal series of coherent spikes of random intensity with essentially 100% fluctuation [43]. This stochastic temporal intensity profile of the pulse creates different gain conditions in the sample, even when the overall peak power of the pulse does not change.

The relative peak position and width (FWHM) of the emission line as a function of the emitted number of photons for the individual shots are shown in Figure 2. The gain and the emission width depend on the exact SASE pulse property of the pump field for a fixed gain-length product, i.e. the exponential amplification factor. Consequently, similar to the observed scatter of intensities shown in Figure 1c, the width of the stimulated emission spectrum for a particular number of output photons shows a strong pulse-to-pulse fluctuation.

The mean value of the peak width as a function of photon number shows an essentially constant line width of 1.9 ± 0.25 eV FWHM extending over the exponential region covering three orders of magnitude up to $2\times10^5$ detected photons (Figure 2 bottom). Note that this observed K$\alpha_1$ line width is much narrower than that of spontaneous emission. To understand this difference, we first describe the contributions to the spontaneous XES spectrum of

$MnCl_2$ shown in Figure 3b. The calculation shows that it consists of multiple final states that contribute to its width of 3.5 eV FWHM. In contrast, in the exponential region of stimulated emission, the strongest emission channel, i.e. the transition to a particular final state with the highest oscillator strength in the spontaneous spectrum, is most likely to be amplified first. This results in an inherent narrowing of the XES spectrum in the exponential regime.

As the number of photons roughly corresponds to the gain-length product, this observation points to the build up of transform limited pulses: Transient amplification schemes, i.e.amplifiers with a rapid gain decay are known to manifest the build-up of transform limited pulses, which has been shown in the quantum treatment of an ideal gain-swept laser by Hopf and Meystre [44]. In a semiclassical treatment of stimulated X-ray emission for a simple two level atomic system [45], it has been numerically demonstrated that the amplification starts with gain narrowing both in the temporal and spectral domain in the first 1-2 gain lengths. After that, transform limited pulses are created that amplify with almost constant pulse profile, until saturation sets in. Our observation of a constant line width of 1.9 eV FWHM includes 0.8 eV instrumental resolution (FWHM). For a Gaussian line profile the real width is therefore ∼1.7 eV FWHM, translating into a pulse duration of ∼1 fs FWHM. Importantly, we also observe spectral widths below the 1.48 eV natural K$\alpha$ lifetime broadening [42] at low peak intensities (Figure 2 bottom), pointing to initial strong gain narrowing at the onset of the exponential region [45]. The narrowest spectrum of stimulated K$\alpha_1$ XES with a bandwidth of 0.95 eV FWHM is shown in Figure 3a, where we fit the data with a pseudo-Voigt with FWHM = 0.8 eV (Gaussian) and 0.5 eV (Lorentzian) for the experimental resolution and the life-time broadening, respectively. Note that previously line widths below the natural lifetime at the onset of the exponential region were only observed by using a second color to seed the amplification [13].

Broadening beyond 1.9 eV and a shift towards lower emission energies can be seen for $> 2 \times 10^5$ detected photons (Figure 2), corresponding to the saturated gain region in Figure 1c. Here, amplification of additional final state intensities occurs leading to a broadening and shift towards lower emission energies, because all the weaker multiplet transitions occur at lower energies (Figure 3b, c). An analogous effect of enhancement of the strongest final-state component and a shift and broadening of the strongest emission line has been predicted previously for vibrational modes [46] in small organic molecules. This interpretation of our observed broadening and shift due to the turning on of additional final states is also supported when comparing K$\alpha_1$ and K$\alpha_2$ emission strengths: In spontaneous emission, the integrated K$\alpha_2$ intensity is approximately half of that of K$\alpha_1$, while it is several orders of magnitude weaker in the exponential region of stimulated emission (see Figures 4 and 3d). It gains strength only after saturation of K$\alpha_1$ has been reached (Figure 3d). A similar observation has been found previously [13]. Our observed initial spectral sharpening, the build-up of bandwidth limited pulses in the exponential gain region, as well as the sequential onset of additional transitions after saturation of the strongest lines (broadening and shift) are unique features of stimulated XES. Note that in the saturation regime, strong-field effects also become increasingly prominent. These can include power broadening and the build up spectral side bands due to Rabi flopping [44, 45]. We provide a simple 3-level ($1s^{-1}$ and $2p_{1/2}^{-1}$ $2p_{3/2}^{-1}$ states) atomic model for Mn in the supporting information, extending previous work [45]. These calculations give a qualitative explanation of the key features of our experimental findings.

To apply stimulated XES for electronic structure analysis, it is critical that its chemical sensitivity is preserved. To address this question, we compare spectra from two systems as shown in Figure 4. In the top panel, stimulated XES spectra in the exponential region of formally $3d^5$ high spin $MnCl_2$ and $3d^0$ $NaMnO_4$ are shown. The spectra were obtained by averaging a number of single shot spectra in the lower exponential region. Comparing the stimulated emission spectra with those from spontaneous emission (middle panel), shows that the stimulated emission spectra are narrower due to gain narrowing and a selection of a subset of transition lines. In addition, a shift in energy of approximately 1.0 eV between $NaMnO_4$ and $MnCl_2$ is observed. This trend agrees with shifts of Mn(VII) and Mn(II) compounds reported in literature [47], as well as with the spontaneous XES data taken at the synchrotron (see Figure 4 (middle)) and theoretical simulations (bottom).

The figure also shows a lack of K$\alpha_2$ intensity in the stimulated XES spectra, as discussed above. However, since the spectra shown in Figure 4 were recorded in the lower exponential region, a weak K$\alpha_2$ signal is still present (see inset). The observed K$\alpha_2$ energy shift between $NaMnO_4$ and $MnCl_2$ is smaller than that of the K$\alpha_1$ emission (0.6 vs 1.0 eV, respectively), which is similar to spontaneous XES. This result is a further indication that the sensitivity to the electronic structure is preserved in stimulated XES despite the very high XFEL pump intensities used.

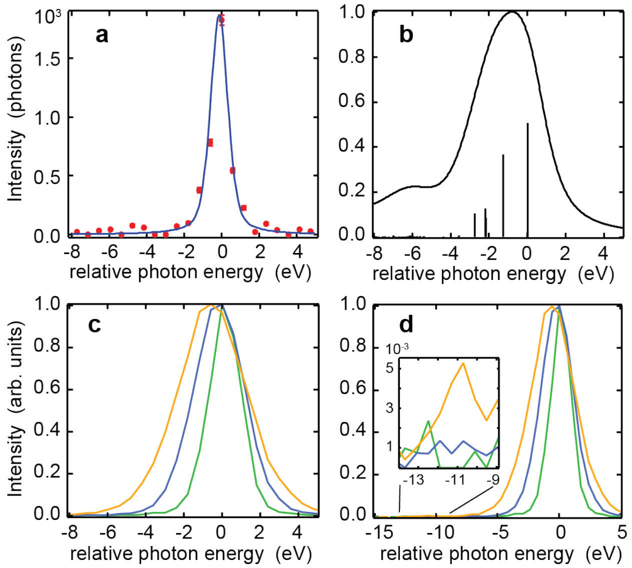

FIG. 3. Line shapes of $MnCl_2$ solution. a: Single shot spectrum together with a pseudo-Voigt fit with FWHM = 0.8 eV (Gaussian) and 0.5 eV (Lorentzian). b: Multiplet simulation of the $MnCl_2$ $K\alpha_1$ line, the vertical sticks represent the intensities at the corresponding final state energies. c: Single shot spectra normalized to maximum with increasing intensity and increasing peak width FWHM = 2.0 (green), 3.1 (blue) and 4.2 eV (yellow), respectively. d: The same as c, but for a wider energy range that also includes the $K\alpha_2$ region. The inset shows a zoom in to the $K\alpha_2$ region with only the widest line carrying intensity.

Yet, it should be noted that the $K\alpha_1$ energy shifts between $NaMnO_4$ and $MnCl_2$ for the stimulated and spontaneous XES spectra are slightly different (see Figure 4). One possible reason for this difference lies in the fact, that for $MnCl_2$ several multiplet lines (see Figures 3 and 4) fall within the natural line width of the common upper lasing state. This couples their oscillator strengths and can lead to shift compared to their natural resonances (see theoretical discussion in the supplementary information). Another possible reason is the ill-defined spatial beam profile in focus. While emission signals along the highest intensity parts of the spatial profile are saturated, showing the strong shift to lower energy, other contributions of lower pump intensity are not saturated. A total average over the focus profile could thus lead to a shift. For a quantitative prediction of this shift, an extended theoretical study is necessary. This is beyond the simple one dimensional gain propagation model presented in the supplementary information and would include treatment of polarization, angular momentum projection of the involved multiplet lines and more accurate calculations

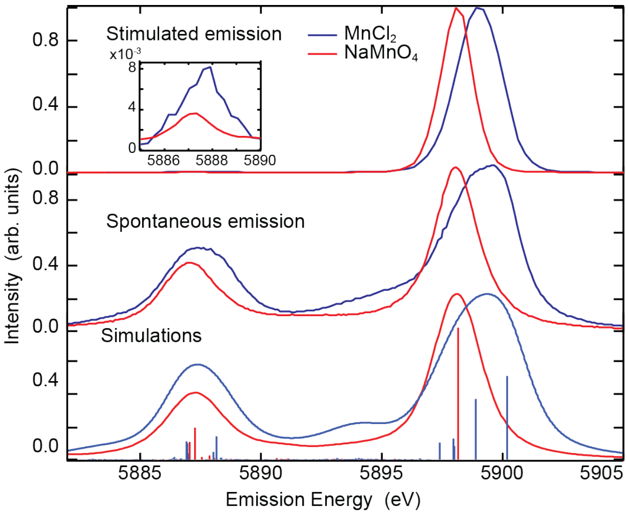

FIG. 4. : Comparison of the averaged stimulated emission spectra of 5M $MnCl_2$ (3773 spectra) and 4M $NaMnO_4$ (3569 spectra) in the lower exponential region (top), and the spontaneous XES spectra taken at SSRL (middle). Note that the presence of a very weak K$\alpha_2$, as shown in the inset, is indicative of weak stimulated XES for these emission channels, far from the saturation regime. Simulations of the spontaneous emission spectra including transitions lines shown as vertical sticks are given in the bottom figure.

of the transition dipoles. Other possible explanations include phenomena such as Auger, ionization and other strong field effects that could in principle lead to a shift mainly for $MnCl_2$ due to its 3d$^5$ electronic configuration. A similar hypothesis for the shift in emission in the Cu experiment upon ionization of 3d electrons was provided previously [13].

To enhance the chemical sensitivity of stimulated XES one can envision using a narrow-band second color beam that co-propagates with the excitation pulse [48] to out-compete the stimulated emission from the strongest channel and selectively amplify weaker multiplet regions that are more chemically sensitive. This, as well as better beam diagnostics and a better theoretical understanding of nonlinear and saturation effects, will help to further disentangle the different spectral contributions and thereby strengthen this new approach.

Use of the Linac Coherent Light Source (LCLS), SLAC National Accelerator Laboratory, is supported by the U.S. Department of Energy, Office of Science, Office of Basic Energy Sciences under Contract No. DE-AC02-76SF00515. Use of the Stanford Synchrotron Radiation Lightsource, SLAC National Accelerator Laboratory, is supported by the U.S. Department of Energy, Office of Science, Office of Basic Energy Sciences under Contract No. DE-AC02-

76SF00515. The SSRL Structural Molecular Biology Program (TK) is supported by the DOE Office of Biological and Environmental Research, and by the National Institutes of Health, National Institute of General Medical Sciences (including P41GM103393). The contents of this publication are solely the responsibility of the authors and do not necessarily represent the official views of NIGMS or NIH. A part of this work was supported by the Director, Office of Science, Office of Basic Energy Sciences (OBES), Division of Chemical Sciences, Geosciences, and Biosciences (CSGB) of the Department of Energy (DOE) (Contract No. DE-AC02-05CH11231, J.Y. and V.K.Y.), National Institutes of Health (NIH) Grants GM055302 (V.K.Y.), GM110501 (J.Y.), the Ruth L. Kirschstein National Research Service Award (F32GM116423, F.D.F.), and the Human Frontiers Science Project Award No. RGP0063/2013 310 (T.F., J.Y., U.B) and the Department of Energy, Laboratory Directed Research and Development program at SLAC National Accelerator Laboratory, under contract DE-AC02-76SF00515 (U.B., Y.Z.). We would like to thank Matt Hayes and the CXI technical staff for experimental support and Gregory Stewart for visual art.

---

* tkroll@slac.stanford.edu

† weninc@slac.stanford.edu

‡ nina.rohringer@desy.de

§ bergmann@slac.stanford.edu

[1] P. Emma, R. Akre, J. Arthur, R. Bionta, C. Bostedt, J. Bozek, A. Brachmann, P. Bucksbaum, R. Coffee, F.-J. Decker, Y. Ding, D. Dowell, S. Edstrom, A. Fisher, J. Frisch, S. Gilevich, J. Hastings, G. Hays, P. Hering, Z. Huang, R. Iverson, H. Loos, M. Messerschmidt, A. Miahnahri, S. Moeller, H.-D. Nuhn, G. Pile, D. Ratner, J. Rzepiela, D. Schultz, T. Smith, P. Stefan, H. Tompkins, J. Turner, J. Welch, W. White, J. Wu, G. Yocky, and J. Galayda, Nat. Photon. **4**, 641 (2010).

[2] T. Ishikawa, H. Aoyagi, T. Asaka, Y. Asano, N. Azumi, T. Bizen, H. Ego, K. Fukami, T. Fukui, Y. Furukawa, S. Goto, H. Hanaki, T. Hara, T. Hasegawa, T. Hatsui, A. Higashiya, T. Hirono, N. Hosoda, M. Ishii, T. Inagaki, Y. Inubushi, T. Itoga, Y. Joti, M. Kago, T. Kameshima, H. Kimura, Y. Kirihara, A. Kiyomichi, T. Kobayashi, C. Kondo, T. Kudo, H. Maesaka, X. M. Maréchal, T. Masuda, S. Matsubara, T. Matsumoto, T. Matsushita, S. Matsui, M. Naga-

sono, N. Nariyama, H. Ohashi, T. Ohata, T. Ohshima, S. Ono, Y. Otake, C. Saji, T. Sakurai, T. Sato, K. Sawada, T. Seike, K. Shirasawa, T. Sugimoto, S. Suzuki, S. Takahashi, H. Takebe, K. Takeshita, K. Tamasaku, H. Tanaka, R. Tanaka, T. Tanaka, T. Togashi, K. Togawa, A. Tokuhisa, H. Tomizawa, K. Tono, S. Wu, M. Yabashi, M. Yamaga, A. Yamashita, K. Yanagida, C. Zhang, T. Shintake, H. Kitamura, and N. Kumagai, Nat. Photon. **6**, 540 (2012).

[3] S. Huang, Y. Ding, Z. Huang, and G. Marcus, Phys. Rev. Accel. Beams **19**, 080702 (2016).

[4] M. W. Guetg, A. A. Lutman, T. J. Ding, Y.and Maxwell, F.-J. Decker, U. Bergmann, and Z. Huang, Phys. Rev. Lett. **120**, 014801 (2018).

[5] W. Zhang, R. Alonso-Mori, U. Bergmann, C. Bressler, M. Chollet, A. Galler, W. Gawelda, R. G. Hadt, R. W. Hartsock, T. Kroll, K. S. Kjær, K. Kubiček, H. T. Lemke, H. W. Liang, D. A. Meyer, M. M. Nielsen, C. Purser, J. S. Robinson, E. I. Solomon, Z. Sun, D. Sokaras, T. B. van Driel, G. Vankó, T.-C. Weng, D. Zhu, and K. J. Gaffney, Nature **509**, 345 (2014).

[6] E. U. Bergmann, V. K. Yachandra, and J. Yano, *X-ray Free Electron Lasers - Applications to Materials, Chemistry and Biology* (Royal Society of Chemistry, 2017).

[7] N. Rohringer and R. Santra, Phys. Rev. A **76**, 033416 (2007).

[8] L. Young, E. P. Kanter, B. Krässig, Y. Li, A. M. March, S. T. Pratt, R. Santra, S. H. Southworth, N. Rohringer, L. F. DiMauro, G. Doumy, C. A. Roedig, N. Berrah, L. Fang, M. Hoener, P. H. Bucksbaum, J. P. Cryan, S. Ghimire, J. M. Glownia, D. A. Reis, J. D. Bozek, C. Bostedt, and M. Messerschmidt, Nature **466**, 56 (2010).

[9] E. P. Kanter, B. Krässig, Y. Li, A. M. March, P. Ho, N. Rohringer, R. Santra, S. H. Southworth, L. F. DiMauro, G. Doumy, C. A. Roedig, N. Berrah, L. Fang, M. Hoener, P. H. Bucksbaum, S. Ghimire, D. A. Reis, J. D. Bozek, C. Bostedt, M. Messerschmidt, and L. Young, Phys. Rev. Lett. **107**, 233001 (2011).

[10] G. Doumy, C. Roedig, S.-K. Son, C. I. Blaga, A. D. DiChiara, R. Santra, N. Berrah, C. Bostedt, J. D. Bozek, P. H. Bucksbaum, J. P. Cryan, L. Fang, S. Ghimire, J. M. Glownia, M. Hoener, E. P. Kanter, B. Krässig, M. Kübel, M. Messerschmidt, G. G. Paulus, D. A. Reis, N. Rohringer, L. Young, P. Agostini, and L. F. DiMauro, Phys. Rev. Lett. **106**, 083002 (2011).

[11] B. Rudek, S.-K. Son, L. Foucar, S. W. Epp, B. Erk, R. Hartmann, M. Adolph, R. Andritschke, A. Aquila, N. Berrah, C. Bostedt, J. Bozek, N. Coppola, F. Filsinger, H. Gorke, T. Gorkhover, H. Graafsma, L. Gumprecht, A. Hartmann, G. Hauser, S. Herrmann, H. Hirse-

mann, P. Holl, A. Hömke, L. Journel, C. Kaiser, N. Kimmel, F. Krasniqi, K.-U. Kühnel, M. Matysek, M. Messerschmidt, D. Miesner, T. Mller, R. Moshammer, K. Nagaya, B. Nilsson, G. Potdevin, D. Pietschner, C. Reich, D. Rupp, G. Schaller, I. Schlichting, C. Schmidt, F. Schopper, S. Schorb, C.-D. Schröter, J. Schulz, M. Simon, H. Soltau, L. Strüder, K. Ueda, G. Weidenspointner, R. Santra, J. Ullrich, A. Rudenko, and D. Rolles, Nature Photonics **6**, 858 (2012).

[12] S. Tanaka and S. Mukamel, Phys. Rev. Lett. **89**, 043001 (2002).

[13] H. Yoneda, Y. Inubushi, K. Nagamine, Y. Michine, H. Ohashi, H. Yumoto, K. Yamauchi, H. Mimura, H. Kitamura, T. Katayama, T. Ishikawa, and M. Yabashi, Nature **524**, 446 (2015).

[14] S. Mukamel, D. M. Healion, Y. Zhang, and J. D. Biggs, Annual Review of Physical Chemistry **64**, 101 (2013).

[15] K. Bennett, Y. Zhang, M. Kowalewski, W. Hua, and S. Mukamel, Physica Scripta **T169**, 014002 (2016).

[16] S. Mukhamel, *Principles of Nonlinear Optical Spectroscopy* (Oxford University Press, 1995).

[17] K. E. Dorfman, Y. Zhang, and S. Mukamel, PNAS **113**, 10001 (2016).

[18] Y. Zhang, J. D. Biggs, N. Govind, and S. Mukamel, J. Phys. Chem. Lett. **5**, 3656 (2014).

[19] G. Vanko, J.-P. Rueff, A. Mattila, Z. Nemeth, and A. Shukla, Phys. Rev. B **73**, 024424 (2006).

[20] P. Glatzel and U. Bergmann, Coord. Chem. Rev. **249**, 65 (2005).

[21] J. A. van Bokhoven and C. Lamberti, *X-Ray Absorption and X-Ray Emission Spectroscopy: Theory and Applications* (Wiley, 2016).

[22] S. DeBeer and U. Bergmann, *X-Ray Emission Spectroscopic Techniques in Bioinorganic Applications in Encyclopedia of Inorganic and Bioinorganic Chemistry, ed R.A. Scott* (John Wiley: Chichester, 2016).

[23] N. Rohringer, D. Ryan, R. A. London, M. Purvis, F. Albert, J. Dunn, J. D. Bozek, C. Bostedt, A. Graf, R. Hill, S. P. Hau-Riege, and J. J. Rocca, Nature **481**, 488 (2012).

[24] C. Weninger, M. Purvis, D. Ryan, R. A. London, J. D. Bozek, C. Bostedt, A. Graf, G. Brown, J. J. Rocca, and N. Rohringer, Phys. Rev. Lett. **111**, 233902 (2013).

[25] M. Beye, S. Schreck, F. Sorgenfrei, C. Trabant, N. Pontius, C. Schüßler-Langeheine, W. Wurth, and A. Föhlisch, Nature **501**, 191 (2013).

[26] V. Kimberg and N. Rohringer, Struct. Dyn. **3**, 034101 (2016).

[27] V. Kimberg, A. Sanchez-Gonzalez, L. Mercadier, C. Weninger, A. Lutman, D. Ratner, R. Coffee, M. Bucher, M. Mucke, M. Agaker, C. Sathe, C. Bostedt, J. Nordgren, R. J. E, and N. Rohringer, Faraday Discuss. **194**, 305 (2016).

[28] M. Liang, G. J. Williams, M. Messerschmidt, M. M. Seibert, P. A. Montanez, M. Hayes, D. Milathianaki, A. Aquila, M. S. Hunter, J. E. Koglin, D. W. Schafer, S. Guillet, A. Busse, R. Bergan, W. Olson, K. Fox, N. Stewart, R. Curtis, A. A. Miahnahri, and S. Boutet, J. Synchrotron Rad. **22** (2015), 10.1073/pnas.1610729113.

[29] B. Nagler, A. Aquila, S. Boutet, E. C. Galtier, A. Hashim, M. S. Hunter, M. Liang, A. E. Sakdinawat, C. G. Schroer, A. Schropp, M. H. Seaberg, F. Seiboth, T. van Driel, Z. Xing, Y. Liu, and H. J. Lee, Scientific Reports **7**, 13698 (2017).

[30] S. Herrmann, S. Boutet, B. Duda, D. Fritz, G. Haller, P. Hart, R. Herbst, C. Kenney, H. Lemke, M. Messerschmidt, J. Pines, A. Robert, M. Sikorski, and G. Williams, Nucl. Instrum. Methods Phys. Res. A **718**, 550 (2013).

[31] D. Sokaras, T.-C. Weng, D. Nordlund, R. Alonso-Mori, P. Velikov, D. Wenger, A. Garachtchenko, M. George, V. Borzenets, B. Johnson, T. Rabedeau, and B. U, Rev. Sci. Instrum. **84**, 053102 (2013).

[32] R. D. Cowan, *The Theory of Atomic Structure and Spectra* (University of California Press: Berkeley, 1981).

[33] P. H. Butler, *Point Group Symmetry: Applications, Methods and Tables* (Plenum Press: New York, 1981).

[34] B. T. Thole, G. van der Laan, J. Fuggle, G. A. Sawatzky, R. C. Karnatak, and J.-M. Esteva, Phys. Rev. B **32**, 5107 (1985).

[35] F. M. F. de Groot and A. Kotani, *Core Level Spectroscopy of Solids* (CRC Press: Boca Raton, FL, 2008).

[36] M. A. Duguay and G. P. Rentzepis, Appl. Phys. Lett. **10**, 350 (1967).

[37] W. H. Louisell, M. O. Scully, and W. B. McKnight, Phys. Rev. A **11**, 989 (1975).

[38] F. A. Hopf and P. Meystre, Phys. Rev. A **12**, 2534 (1975).

[39] F. A. Hopf, Optics Letters **7**, 605 (1982).

[40] Self-seeded stimulated emission is also sometimes referred to as 'amplified spontaneous emission' (ASE). Throughout the paper we refer to it simply as 'stimulated emission'.

[41] N. Rohringer and R. London, Phys. Rev. A **80**, 013809 (2009).

[42] M. O. Krause and J. H. Oliver, Journal of Physical and Chemical Reference Data **8**, 329 (1979).

[43] S. Krinsky and R. L. Gluckstern, Phys. Rev. ST Accel. Beams **6**, 050701 (2003).

[44] F. A. Hopf and P. Meystre, Phys. Rev. A **12**, 2534 (1975).

[45] C. Weninger and N. Rohringer, Phys. Rev. A **90**, 063828 (2014).

[46] V. Kimberg and N. Rohringer, Phys. Rev. Lett. **110**, 043901 (2013).

[47] U. Bergmann and P. Glatzel, Photosynthesis Research **102**, 255 (2009).

[48] A. A. Lutman, R. Coffee, Y. Ding, Z. Huang, J. Krzywinski, T. Maxwell, M. Messerschmidt, and H.-D. Nuhn, Phys. Rev. Lett. **110**, 134801 (2013).